Nonredundant roles of cytoplasmic β- and γ-actin isoforms in regulation of epithelial apical junctions

Somesh Baranwal[a,b], Nayden G. Naydenov[a,b], Gianni Harris[a], Vera Dugina[c], Kathleen G. Morgan[d], Christine Chaponnier[c], and Andrei I. Ivanov[a,b]

[a]Department of Medicine, University of Rochester, Rochester, NY 14642; [b]Department of Human and Molecular Genetics and Virginia Institute of Molecular Medicine, Virginia Commonwealth University, Richmond, VA 23298; [c]Department of Pathology and Immunology, Centre Medical Universitaire, University of Geneva, Geneva 4, Switzerland; [d]Department of Health Sciences, Boston University, Boston, MA 02215

ABSTRACT **Association with the actin cytoskeleton is critical for normal architecture and dynamics of epithelial tight junctions (TJs) and adherens junctions (AJs). Epithelial cells express β-cytoplasmic (β-CYA) and γ-cytoplasmic (γ-CYA) actins, which have different cellular localization and functions. This study elucidates the roles of cytoplasmic actins in regulating structure and remodeling of AJs and TJs in model intestinal epithelia. Immunofluorescence labeling and latrunculin B treatment reveal affiliation of dynamic β-CYA filaments with newly assembled and mature AJs, whereas an apical γ-CYA pool is composed of stable perijunctional bundles and rapidly turning-over nonjunctional filaments. The functional effects of cytoplasmic actins on epithelial junctions are examined by using isoform-specific small interfering RNAs and cell-permeable inhibitory peptides. These experiments demonstrate unique roles of β-CYA and γ-CYA in regulating the steady-state integrity of AJs and TJs, respectively. Furthermore, β-CYA is selectively involved in establishment of apicobasal cell polarity. Both actin isoforms are essential for normal barrier function of epithelial monolayers, rapid AJ/TJ reassembly, and formation of three-dimensional cysts. Cytoplasmic actin isoforms play unique roles in regulating structure and permeability of epithelial junctions.**

Monitoring Editor
Richard Fehon
University of Chicago

Received: Feb 27, 2012
Revised: Jul 16, 2012
Accepted: Jul 24, 2012

INTRODUCTION

Barrier function and morphogenic plasticity of metazoan epithelia depend on elaborate adhesive contacts between adjacent epithelial cells. These intercellular contacts are composed of several types of multiprotein complexes at the plasma membrane called junctions (Giepmans and van Ijzendoorn, 2009; Green *et al.*, 2010). In simple epithelia, closest to the luminal surface, tight junctions (TJs) and underlying adherens junctions (AJs) form an apical junctional complex (AJC) that plays key roles in regulating integrity and permeability of epithelial monolayers (Gumbiner, 2005; Shin *et al.*, 2006; Hartsock and Nelson, 2008; Niessen *et al.*, 2011). Adhesive properties of TJs and AJs are determined by integral membrane proteins associated with cytoplasmic scaffolds. Occludin, claudins, and junctional adhesion molecule A are major transmembrane components of TJs interacting with members of the zonula occludens (ZO) protein family (Hartsock and Nelson, 2008; Anderson and Van Itallie, 2009; Shen *et al.*, 2011). Adhesive properties of epithelial AJs are determined by E-cadherin, which binds to cytoplasmic α, β, and p120 catenins (Gumbiner, 2005; Hartsock and Nelson, 2008; Niessen *et al.*, 2011).

Molecular organization of the epithelial AJC relies on a delicate balance of adhesive strength and structural plasticity (Ivanov, 2008; Cavey and Lecuit, 2009; Niessen *et al.*, 2011; Shen *et al.*, 2011). The former feature allows cells to withstand a variety of mechanical and osmotic stresses and is important for epithelial integrity and barrier function. The latter feature permits rapid remodeling of epithelial cell–cell contacts during embryonic morphogenesis and mucosal

This article was published online ahead of print in MBoC in Press (http://www.molbiolcell.org/cgi/doi/10.1091/mbc.E12-02-0162) on August 1, 2012.

Address correspondence to: Andrei I. Ivanov (aivanov2@vcu.edu).

Abbreviations used: AJ, adherens junction; AJC, apical junctional complex; aPKC, atypical protein kinase C; β-CYA, β-cytoplasmic actin; γ-CYA, γ-cytoplasmic actin; MLC, myosin light chain; NM II, nonmuscle myosin II; siRNA, small interfering RNA; α-SMA, α-smooth muscle actin; TEER, transepithelial electrical resistance; TJ, tight junction; ZO, zonula occludens.

restitution. It is generally believed that this combination of AJC strength and plasticity is determined by interactions between junctional complexes and the underlying actin cytoskeleton (Mege *et al.*, 2006; Ivanov, 2008; Cavey and Lecuit, 2009; Meng and Takeichi, 2009).

A crucial role of actin filaments in regulation of AJs and TJs is supported by several lines of evidence. First, initial pharmacological experiments observed that actin-depolymerizing fungal toxins—cytochalasins—potently disrupted epithelial barriers (Bentzel *et al.*, 1980; Madara *et al.*, 1986). Second, subsequent ultrastructural studies revealed a complex perijunctional actin cytoskeleton composed of the AJ-associated circumferential F-actin belt (Hirokawa and Tilney, 1982; Hirokawa *et al.*, 1983) and TJ-associated network of F-actin bundles (Madara, 1987). Finally, recent genetic approaches identified a number of actin-polymerizing, bundling, and motor proteins affiliated with either AJs or TJs and demonstrated their roles in regulating AJC structure and function (Mege *et al.*, 2006; Ivanov, 2008; Meng and Takeichi, 2009; Niessen *et al.*, 2011). Of importance, disruption of actin filaments is known to impair all major stages of AJC biogenesis, including the maintenance of mature AJs and TJs (Madara *et al.*, 1986; Volberg *et al.*, 1986; Ma *et al.*, 1995; Shen and Turner, 2005), rapid AJ/TJ disassembly (Ma *et al.*, 2000; Ivanov *et al.*, 2004), and reestablishment of intercellular contacts (Vasioukhin *et al.*, 2000; Ivanov *et al.*, 2005; Zhang *et al.*, 2005). However, molecular details of these critical interactions between the epithelial AJC and the perijunctional actin cytoskeleton remain incompletely understood.

One of the most interesting features of AJ/TJ-associated actin filaments is their structural heterogeneity. For example, de novo assembly of epithelial junction is coupled with dramatic transformation of the perpendicular F-actin cables supporting nascent cell–cell contacts into the circumferential F-actin belt associated with the mature AJC (Yonemura *et al.*, 1995; Yonemura, 2010; Vasioukhin *et al.*, 2000; Ivanov *et al.*, 2005; Taguchi *et al.*, 2011). Conversely, rapid junctional disassembly is accompanied by replacement of the perijunctional F-actin belt with radial retraction fibers (Ma *et al.*, 2000; Ivanov *et al.*, 2004). Actin filaments appear to be heterogeneous even at the same stage of the AJC biogenesis. For instance, two F-actin pools were observed at E-cadherin–based cell–cell junctions in *Drosophila* embryo: a small pool of stable filaments associated with E-cadherin clusters and a larger pool of rapidly turning-over contractile filaments (Cavey *et al.*, 2008). Similarly, stable and unstable F-actin structures were implicated in formation of cell–cell contacts between differentiating keratinocytes (Zhang *et al.*, 2005). The molecular nature of these distinct junction-associated F-actin pools remains unknown. Some studies suggested that different occupancy of actin filaments by various accessory proteins can originate and maintain such heterogeneity (Abe and Takeichi, 2008; Smutny *et al.*, 2010; Taguchi *et al.*, 2011). However, it is equally possible that the cytoskeletal heterogeneity can be determined by different biochemical properties of actin polymers per se.

Epithelial cells express two different actin isoforms known as cytoplasmic β- and γ- actins (β-CYA and γ-CYA, respectively). These isoforms have nearly identical sequences and differ only in four amino acids in a close vicinity of their N-terminus (Vandekerckhove and Weber, 1978; Khaitlina, 2001; Perrin and Ervasti, 2010). Despite such remarkable similarity, β-CYA and γ-CYA have different kinetics of polymerization in vitro (Bergeron *et al.*, 2010) and different intracellular localization (Micheva *et al.*, 1998; Belyantseva *et al.*, 2009; Dugina *et al.*, 2009; Tondeleir *et al.*, 2009), all of which points to possible unique functions of cytoplasmic actins. In line with this suggestion, an early overexpression study demonstrated distinct effects of β-CYA and γ-CYA on cellular morphology of myoblasts (Schevzov *et al.*, 1992), whereas recent gene-knockout experiments revealed nonredundant roles of β-CYA and γ-CYA in regulating cell growth, motility, and organization of the intracellular cytoskeleton (Belyantseva *et al.*, 2009; Bunnell and Ervasti, 2010; Bunnell *et al.*, 2011; Perrin *et al.*, 2010). Nevertheless, the functional effects of cytoplasmic actin isoforms on the epithelial AJC have not been previously investigated. This study dissects the roles of β-CYA and γ-CYA in regulating structure, dynamics, and functions of TJs and AJs in model intestinal epithelia.

RESULTS

β-CYA and γ-CYA demonstrated differential localization and dynamics at epithelial junctions

In spite of previous reports that visualized both β-CYA and γ-CYA at the apex of polarized epithelial cells in close proximity to intercellular contacts (Yao *et al.*, 1995; Dugina *et al.*, 2008, 2009), it remains unknown which cytoplasmic actin is associated with the AJC. To answer this question, we performed immunolabeling of β-CYA or γ-CYA with β-catenin and ZO-1, which are known protein markers of AJs and TJs, respectively. A calcium switch model was used to examine F-actin structures affiliated with initial intercellular contacts and the mature AJC in SK-CO15 human colonic epithelial cell monolayers. After 1 h of calcium repletion, SK-CO15 cells rapidly assembled nascent AJs, which were characterized by either dot-like or continuous β-catenin labeling at the areas of cell–cell contacts (Figure 1A). β-CYA bundles were enriched in very close proximity of these nascent AJs and significantly colocalized with β-catenin (Figure 1A, arrows). By contrast, γ-CYA–rich filaments localized behind newly assembled intercellular junctions and showed little colocalization with β-catenin (arrowheads). After 24 h of calcium repletion, β-CYA appeared to be associated with mature AJs and TJs, based on its colocalization with both ZO-1 (Figure 1B, arrows) and β-catenin (Supplemental Figure S1). On the other hand, γ-CYA was uniformly distributed at the cell apex without showing specific enrichment at apical junctions (Figure 1B, arrowheads, and Supplemental Figure S1). Of interest, removal of monomeric actin by preextracting live SK-CO15 cells with Triton X-100 exposed perijunctional γ-CYA–labeled structures (Supplemental Figure S2), which suggests the existence of AJC-associated pools of both cytoplasmic actins.

We next sought to investigate the dynamic properties of these perijunctional fractions of β-CYA and γ-CYA by probing their sensitivity to latrunculin B (Lat B) treatment (Ammar *et al.*, 2001; Ivanov *et al.*, 2005; Abe and Takeichi, 2008). Lat B is known to specifically bind and sequester monomeric actin, which triggers preferential depolymerization of rapidly turning-over actin filaments (Ayscough, 1998; Morton *et al.*, 2000). Exposure of confluent SK-CO15 cells to Lat B (1 μM for 1 h) resulted in a significant decrease in β-CYA labeling at apical junctions, which was accompanied by disintegration of β-catenin–based AJs (Figure 2A, arrows). By contrast, Lat B treatment dramatically transformed a diffuse apical γ-CYA labeling into a sharp perijunctional staining colocalized with ZO-1 (Figure 2B, arrowheads). Phalloidin labeling of Lat B–treated SK-CO15 cells also revealed an intact perijunctional F-actin belt that was identical to γ-CYA–labeled bundles (unpublished data). These results can be explained by the existence of two pools of γ-CYA–based filaments at the cell apex: slowly turning-over AJC-associated bundles and rapidly turning-over nonjunctional filaments. Lat B exposure caused disassembly of these nonjunctional γ-CYA filaments, thereby unmasking stable AJC-associated bundles. Overall our data suggest that both cytoplasmic actin isoforms are present at the epithelial AJC, although junction-associated pools of β-CYA and γ-CYA have

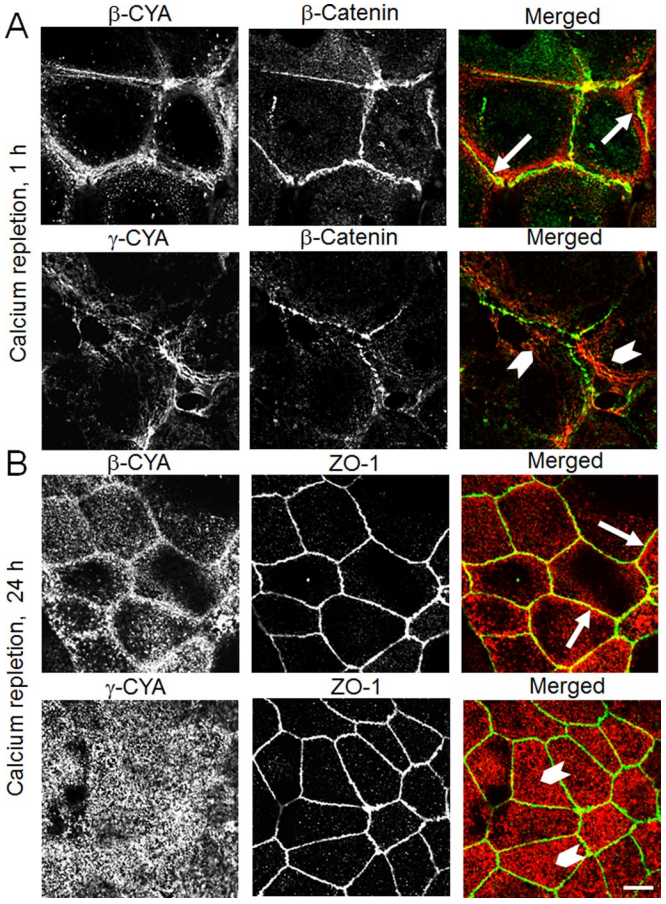

FIGURE 1: β-CYA is selectively enriched at newly formed epithelial junctions and the mature AJC. Confluent SK-CO15 cells were subjected to overnight extracellular calcium depletion to disassemble intercellular contacts, followed by either 1 (A) or 24 (B) h of calcium repletion to induce junctional reassembly. Cells were fixed and subjected to dual immunolabeling for either β-CYA or γ-CYA (red) with β-catenin and ZO-1 (green). Representative confocal images show accumulation of β-CYA at newly assembled junctions and the mature AJC (arrows) and lack of colocalization of junctional proteins with γ-CYA (arrowheads). Scale bar, 5 μm.

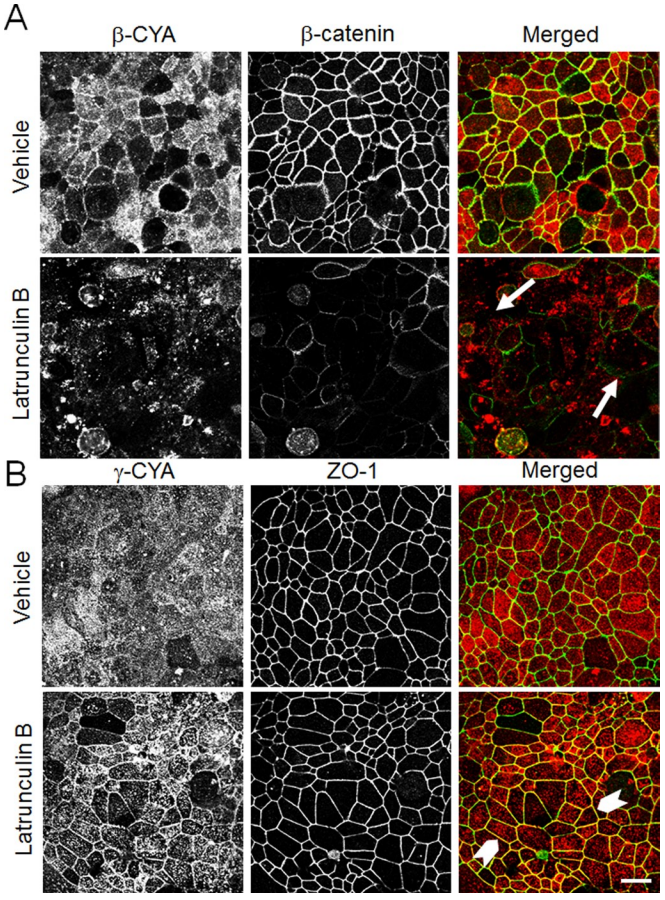

FIGURE 2: Apical β-CYA or γ-CYA structures have different sensitivity to latrunculin-induced F-actin depolymerization. Confluent SK-CO15 cell monolayers were incubated for 1 h with either vehicle or latrunculin B (1 μM). Cells were fixed and immunolabeled for cytoplasmic actins (red) and junctional protein (green). Note that latrunculin B treatment disrupted β-CYA labeling at apical junctions (arrows) but enhanced AJC localization of γ-CYA (arrowheads). Scale bar, 20 μm.

different dynamics and are recruited at different times of AJC assembly.

Down-regulation of β-CYA and γ-CYA differently affected maintenance of AJs and TJs and apicobasal cell polarity

To examine the roles of β-CYA and γ-CYA in the regulation of epithelial junctions, we depleted these actin isoforms in SK-CO15 cells by RNA interference. Two different β-CYA–specific or γ-CYA–specific small interfering RNA (siRNA) duplexes decreased expression of these proteins by up to 98 and 79%, respectively, on day 4 posttransfection (Figure 3A). Of interest, depletion of individual cytoplasmic actins caused compensatory up-regulation of the remaining isoform. For example, down-regulation of β-CYA resulted in an ~17% increase in γ-CYA expression, whereas γ-CYA knockdown triggered an ~65% increase in β-CYA level (Figure 3A). As a result, loss of β-CYA markedly (by ~50%) reduced total level of actin, whereas depletion of γ-CYA caused just a modest (<20%) decrease in the total actin content (Figure 3A). Depletion of neither cytoplasmic actin induced cell apoptosis as indicated by the absence of PARP cleavage and caspase activation (Figure 3B). This result is consistent with a reported lack of toxicity of β-CYA siRNA in HeLa cells (Liu *et al.*, 2007), but contradicts the proapoptotic effects of β-CYA and γ-CYA knockdown in mouse embryonic fibroblasts (Bunnell and Ervasti, 2010; Bunnell *et al.*, 2011).

Of importance, down-regulation of either cytoplasmic actin markedly impaired barrier properties of the model intestinal epithelia. Indeed, control siRNA–treated SK-CO15 cell monolayers rapidly developed high transepithelial electrical resistance (TEER), which reached ~1600 Ω cm^2 on day 4 posttransfection (Figure 3C). By contrast, β-CYA– or γ-CYA–depleted cell monolayers showed significantly lower TEER, which reached only ~240 and 170 Ω cm^2, respectively (Figure 3C). Similar results were obtained with HT-29 cF8 intestinal epithelial cells (unpublished data). To examine whether loss of cytoplasmic actin isoforms also affected permeability to large uncharged molecules, we measured transepithelial passage of fluoresceinated dextrans with molecular masses of 4 and 40 kDa (Figure 3D). Depletion of either β-CYA or γ-CYA significantly increased dextran fluxes in SK-CO15 cell monolayers on day 4 posttransfection (Figure 3D). Collectively these data suggest that both cytoplasmic actins are essential for normal barrier function in the model intestinal epithelia.

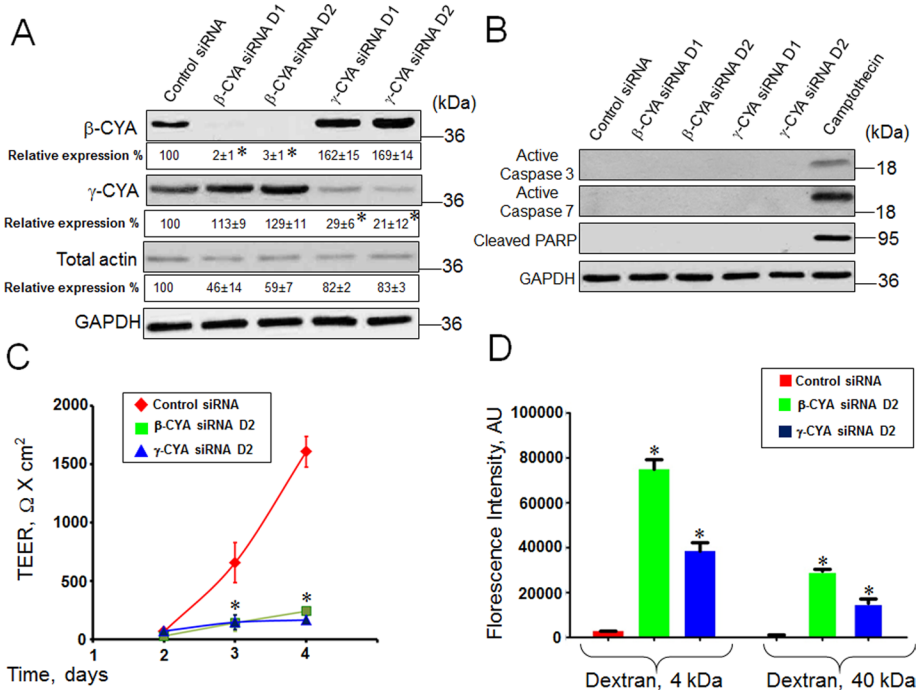

FIGURE 3: Down-regulation of β-CYA and γ-CYA attenuates formation of the paracellular barrier in apoptosis-independent manner. SK-CO15 cells were transfected with control, β-CYA–, or γ-CYA–specific siRNAs, and development of the paracellular barrier was examined by measuring TEER and fluoresceinated dextran flux. (A, B) Immunoblotting analysis shows a selective down-regulation of individual cytoplasmic actins on day 4 posttransfection, which differently affects the total actin level and does not stimulate apoptotic events such as PARP cleavage or caspases activation. Camptothecin treatment (10 μM for 24 h) is shown as a positive control for apoptosis. (C, D) Permeability assays reveal significant attenuation of TEER development and increased dextran fluxes in β-CYA– or γ-CYA–depleted cell monolayers on day 4 posttransfection. Data are presented as mean ± SE ($n = 3$); *$p < 0.05$, compared to control siRNA–transfected cells.

We next sought to investigate whether the increased permeability of β-CYA– and γ-CYA–depleted epithelial cell monolayers was associated with the impaired structure of apical junctions. Immunofluorescence labeling and confocal microscopy allowed us to easily visualize the areas of cell monolayers depleted of cytoplasmic actins, which were characterized not only by loss of either β-CYA or γ-CYA labeling intensity, but also by a marked increase in the cell size (Figures 4 and 5). We found that β-CYA depletion in SK-CO15 cells dramatically disrupted AJ structure, which was manifested by redistribution of β-catenin from the areas of cell–cell contact (Figure 4A, arrows) to the cytoplasmic and nuclear compartments (Figure 4A, arrowheads). Similar effects were observed after immunolabeling of other AJ proteins, E-cadherin and α-catenin (Supplemental Figure S3, arrowheads). Surprisingly, β-CYA knockdown did not alter TJ integrity, as evident from intact junctional staining of ZO-1 (Figure 4B, arrows), occludin, and claudin-1 (Supplemental Figure S3, arrows). Down-regulation of γ-CYA expression had a different effect on the AJC. This knockdown did not alter AJ structure (Figure 5A and Supplemental Figure S3, arrows) but resulted in defective junctional labeling of ZO-1 (Figure 5B, arrowheads), occludin, and claudin-1 (Supplemental Figure S3, arrowheads), thereby indicating the impaired TJ integrity. Immunoblotting analysis showed that the observed changes of AJ and TJ structure in actin isoform–depleted cells were not due to decreased expression of major AJC proteins (Supplemental Figure S4).

Given the intimate relationships between epithelial apical junctions and apicobasal cell polarity (Shin *et al.*, 2006; McCaffrey and Macara, 2009), we examined whether the impaired junctional architecture in β-CYA and γ-CYA knockdowns was accompanied by altered cell polarity. Control siRNA–treated SK-CO15 cells growing on membrane filters became well polarized on day 4 posttransfection, as indicated by a defined apical plasma membrane labeling of EBP50 protein and lateral plasma membrane localization of β-catenin (Figure 6A). Such polarity was largely preserved in γ-CYA–depleted cells but was disrupted after β-CYA knockdown, leading to diffuse intracellular labeling of EBP50 and mislocalization of β-catenin to the cell apex (Figure 6A). Because epithelial cell polarity is regulated by the Par-3–Par-6-atypical protein kinase C (aPKC) polarity complex (Suzuki and Ohno, 2006; McCaffrey and Macara, 2009), we next examined the effects of actin isoform knockdown on expression and activation of key molecular constituents of this complex. Immunoblotting analysis demonstrated that neither β-CYA nor γ-CYA depletion altered protein expression of Par-3, Par-6, and two major aPKC isoforms, ζ and ι, in SK-CO15 cells (Figure 6B). Furthermore, actin isoform knockdown did not affect the cellular level of phosphorylated (active) aPKCζ and aPKCι. Of interest, impaired recruitment of Par-3 to AJC was found in SK-CO15 cells after β-CYA knockdown (Figure 6C, arrowheads), which indicates that mislocalization of the Par-3–Par-6–aPKC complex can contribute to the observed defects of he apicobasal cell polarity after β-CYA depletion. Overall our data revealed that β-CYA and γ-CYA play different roles in controlling steady-state structure of AJs and TJs and cooperate in regulating the barrier properties of epithelial cell monolayers.

Inhibition of β-CYA and γ-CYA attenuated reassembly of epithelial apical junctions

Given the known ability of the epithelial AJC to undergo cytoskeleton-dependent disassembly and reassembly (Mege *et al.*, 2006; Ivanov, 2008; Yonemura, 2010), we sought to investigate how such junctional remodeling is regulated by two cytoplasmic actins. Extracellular calcium depletion was used to trigger AJ and TJ disassembly in SK-CO15 cell monolayers. This procedure caused a rapid (within 1 h) loss of ZO-1 (Supplemental Figure S5) and β-catenin (Supplemental Figure S6) from the majority of cell–cell contacts. Similarly, calcium depletion induced a dramatic reorganization of β-CYA and γ-CYA into apical ring-like structures (Supplemental Figure S5). Of importance, both cytoplasmic actins demonstrated very similar labeling patterns in calcium-depleted epithelia, being enriched at disassembling apical junctions (Supplemental Figure S5, arrows). Down-regulation of either β-CYA or γ-CYA expression did not affect disruption of AJs and TJs as compared with control siRNA–treated SK-CO15 cells (Supplemental Figure S6 and unpublished data). Collectively, these results indicate the redundant roles of these actin isoforms during rapid disintegration of epithelial apical junctions.

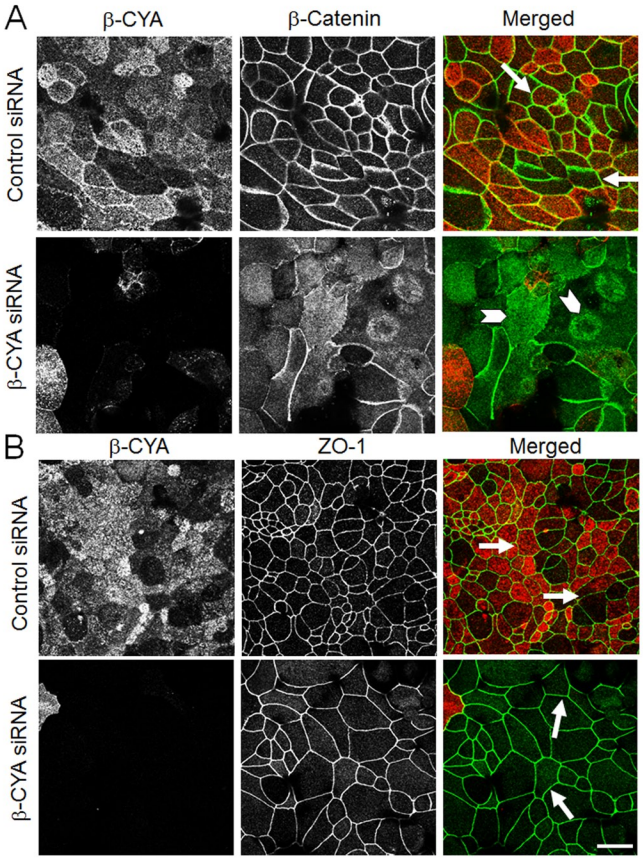

FIGURE 4: Down-regulation of β-CYA expression selectively disrupts the organization of mature AJs. SK-CO15 cells were transfected with either control or β-CYA–specific siRNAs, and the integrity of their AJs and TJs was examined by immunolabeling and confocal microscopy on day 4 posttransfection. Note that β-CYA depletion transforms junctional labeling of β-catenin (A, arrows) into a diffuse intracellular staining (arrowheads) but does not affect normal ZO-1 labeling at TJs (B, arrows). Scale bar, 20 μm.

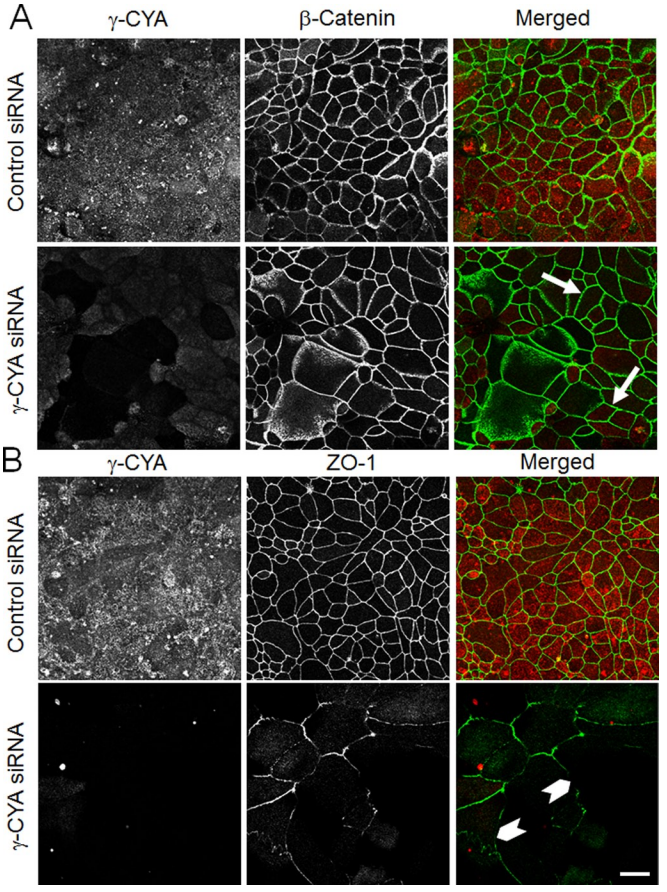

FIGURE 5: Down-regulation of γ-CYA expression selectively impairs maintenance of TJs. SK-CO15 cells were transfected with either control or γ-CYA–specific siRNAs, and the integrity of their AJs and TJs was examined by immunolabeling and confocal microscopy on day 4 posttransfection. Note that depletion of γ-CYA disrupts ZO-1 labeling at TJs (arrowheads) without affecting β-catenin localization at mature AJs (arrows). Scale bar, 20 μm.

We next asked which cytoplasmic actin regulates calcium-dependent reassembly of AJs and TJs. SK-CO15 cells were transfected with control, β-CYA–, or γ-CYA–specific siRNAs, and on day 3 posttransfection they were subjected to overnight calcium depletion followed by readdition of calcium for either 1 or 3 h. In control cell monolayers, calcium repletion caused a rapid accumulation of β-catenin at the intercellular contacts (Figure 7A, arrows), thereby indicating AJ reassembly. By contrast, β-catenin remained intracellularly and did not translocate to the cell–cell contact zone in β-CYA–depleted epithelium (Figure 7A, arrowheads). After 3 h of calcium repletion, control SK-CO15 cells demonstrated a "chicken wire" labeling pattern for ZO-1 (Figure 7B, arrows) that is characteristic for normal TJs. However, β-CYA–deficient cell monolayers revealed only fragmented and disconnected areas of ZO-1 labeling at TJs (Figure 7B, arrowheads). Remarkably, down-regulation of γ-CYA had similar inhibitory effects on AJC reassembly by attenuating calcium-dependent reformation of both AJs and TJs (Figure 8, arrowheads). We sought to confirm these results by another experimental approach involving inhibitory peptides targeting different actin isoforms. This approach was previously used to study actin-dependent contractile processes in myofibroblasts (Hinz *et al.*, 2002) and isolated aorta (Kim *et al.*, 2008). SK-CO15 cells were subjected to 3 h of calcium repletion in the presence of cell-permeable fluorescein isothiocyanate (FITC)–labeled peptides against either β-CYA or γ-CYA and reassembly of their AJC was compared with those in two different controls, one without peptides and the other with a peptide against α-smooth muscle actin (α-SMA), which is not expressed in intestinal epithelial cells. The peptide-free and α-SMA peptide–treated controls show a substantial reassembly of β-catenin–based AJs and ZO-1–based TJs (Supplemental Figures S7 and S8, arrows). By contrast, addition of either β-CYA or γ-CYA peptides significantly attenuates such AJ/TJ reassembly (Supplemental Figures S7 and S8, arrowheads), thereby reinforcing the results of the RNA interference experiments. Overall these data suggest that cytoplasmic actin isoforms may play distinct and redundant roles at different steps of AJC remodeling.

Down-regulation of β-CYA and γ-CYA attenuated reassembly of the perijunctional actomyosin belt

Because re-formation of epithelial AJs and TJs critically depends on the assembly of the apical circumferential actin belt containing activated nonmuscle myosin II (NM II) motor (Ivanov *et al.*, 2005, 2007; Shewan *et al.*, 2005; Zhang *et al.*, 2005; Smutny *et al.*, 2010), one can expect that depletion of β-CYA or γ-CYA attenuated AJ/TJ reassembly by impairing formation of such perijunctional actomyosin cytoskeleton. To test this idea, we visualized actin filaments at the

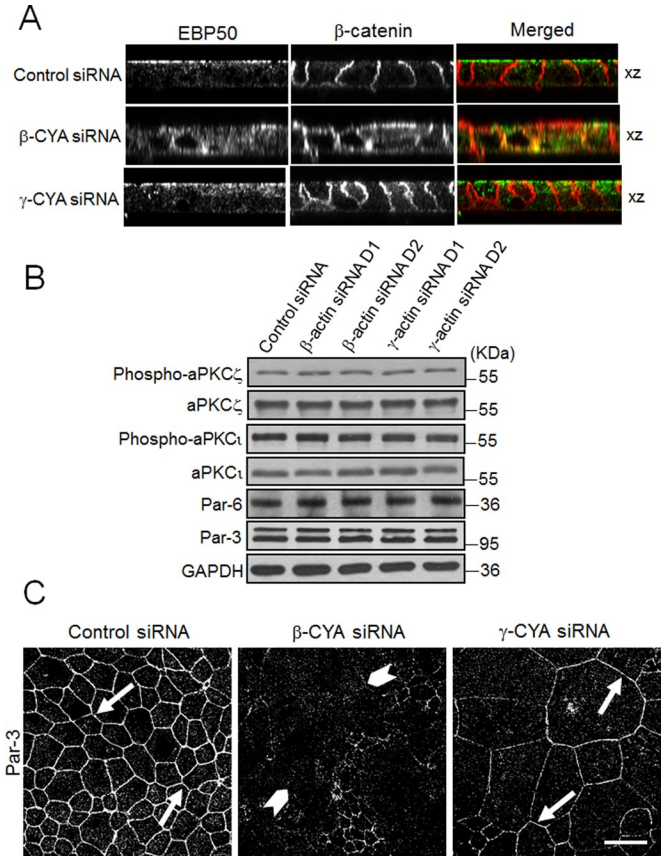

FIGURE 6: Down-regulation of β-CYA selectively impairs apicobasal cell polarity. (A) Reconstructed *xz* confocal images show proper localization of apical plasma membrane marker EBP50 (red) and basolateral membrane marker β-catenin (green) in control and γ-CYA–depleted SK-CO15 cells. By contrast, β-CYA–knockdown cells demonstrate diffuse intracellular staining of the apical plasma membrane marker. (B) Immunoblotting analysis shows that knockdown of β-CYA or γ-CYA did not affect expression of molecular constituents of the Par3–Par6–aPKC polarity complex, as well as phosphorylation of two aPKC isoforms. (C) Immunofluorescence images show junctional localization of Par-3 in control and γ-CYA–depleted cells (arrows) and mislocalization of Par-3 in β-CYA knockdown (arrowheads). Scale bar, 20 μm.

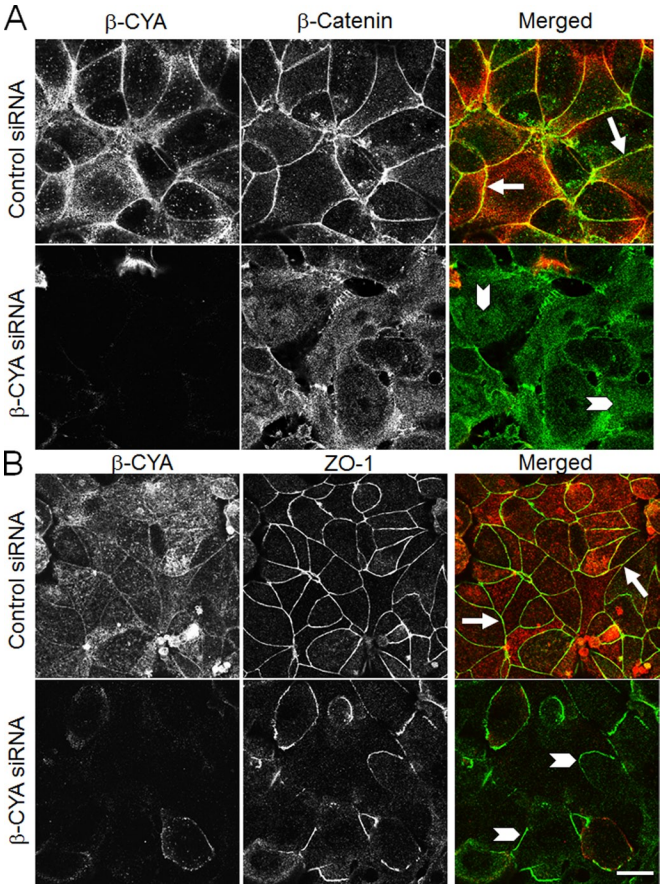

FIGURE 7: Down-regulation of β-CYA expression attenuates reassembly of AJs and TJs. Reassembly of AJs and TJs was examined in control and β-CYA–depleted SK-CO15 cells after 1 (A) or 3 (B) h of calcium repletion. Immunofluorescence labeling and confocal microscopy demonstrate accumulation of the majority of β-catenin and ZO-1 at the intercellular contacts in control cell monolayers (arrows), whereas in β-CYA–deficient cells a substantial amount of β-catenin remains in the cytoplasm and only short, defective ZO-1–based TJs are formed (arrowheads). Scale bar, 20 μm.

newly forming epithelial cell–cell contacts by using fluorescently labeled phalloidin. After 3 h of calcium repletion, control SK-CO15 cells assembled a well-defined perijunctional F-actin belt (Figure 9, A and B, arrows). By contrast, β-CYA– (Figure 9A) or γ-CYA–deficient cell monolayers (Figure 9B) demonstrated the diminished intensity and thickness of these circumferential F-actin bundles (Figure 9, A and B, arrowheads). Similar results were obtained by using β-CYA and γ-CYA inhibitory peptides. These peptides selectively perturbed labeling of the targeted actin isoform but similarly decreased intensity of perijunctional actin filaments (Supplemental Figure S9, arrows). To examine contractile properties of the AJC-associated cytoskeleton in cytoplasmic actin-depleted epithelia, we used immunolabeling of phosphorylated myosin light chain (p-MLC), a classic marker of NM II activation (Matsumura, 2005; Vicente-Manzanares *et al.*, 2009). Control SK-CO15 cells showed significant accumulation of p-MLC at newly-formed TJs after 3 h of calcium repletion (Figure 10A, arrows). By contrast, junctional p-MLC labeling was barely detectable in β-CYA– and γ-CYA–depleted cells (arrowheads). Furthermore, immunoblotting analysis revealed that knockdown of either cytoplasmic actin isoform resulted in up to 50% decrease in the cellular level of p-MLC without altering expression of total MLC (Figure 10B). Expression of NM II heavy-chain isoforms A–C was not changed in either β-CYA– or γ-CYA–depleted cells (Figure 10B). Taken together, these results suggest that defective formation of the circumferential F-actin belt and decreased activation of perijunctional NM II may be responsible for the attenuated reassembly of AJs and TJs in cytoplasmic actin–depleted epithelial cells.

Loss of cytoplasmic actin isoforms inhibited formation of three-dimensional epithelial cysts

Although epithelial cell monolayers growing on planar matrices (membranes or cover slips) are considered as good in vitro models to study regulation of apical junctions, these models do not recapitulate all aspects of the three-dimensional (3D) epithelial morphogenesis in vivo. Therefore we sought to examine morphogenic roles of cytoplasmic actins by using a Matrigel model of epithelial cystogenesis. For this part of the study, we selected Caco-2 BBE human intestinal epithelial cells, which are known to create cysts with a well-defined lumen after embedding into Matrigel (Ivanov *et al.*, 2008; Durgan *et al.*, 2011). By contrast, Matrigel-growing SK-CO15 cells form

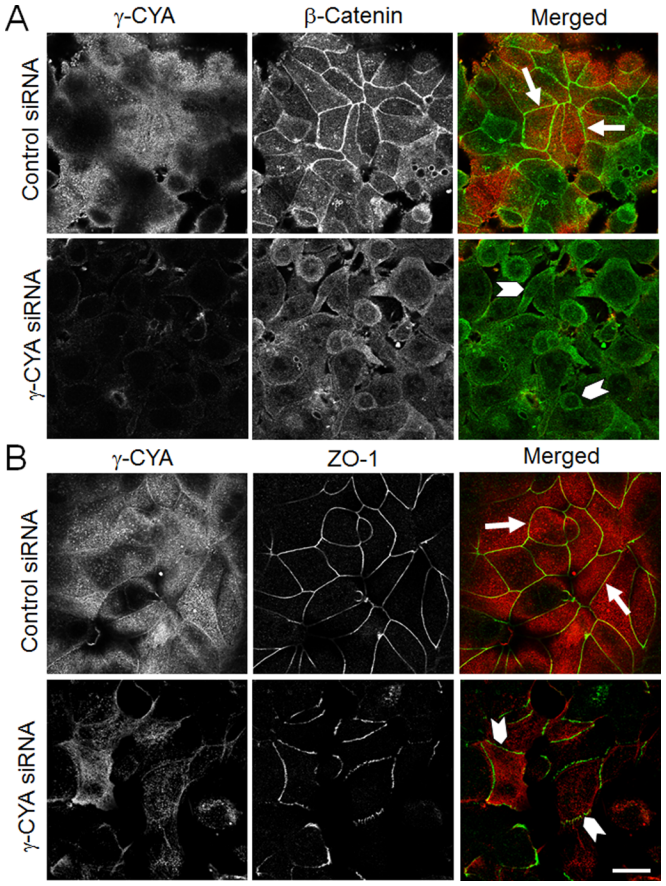

FIGURE 8: Down-regulation of γ-CYA expression attenuates reassembly of AJs and TJs. Junctional reassembly was examined in control and γ-CYA–depleted SK-CO15 cells after 1 (A) or 3 (B) h of calcium repletion. Immunofluorescence labeling and confocal microscopy show reassembly of the majority of β-catenin–based AJs and ZO-1–based TJs in control cell monolayers (arrows). By contrast, γ-CYA–deficient cells demonstrate only short, discontinuous AJs and TJs (arrowheads). Scale bar, 20 μm.

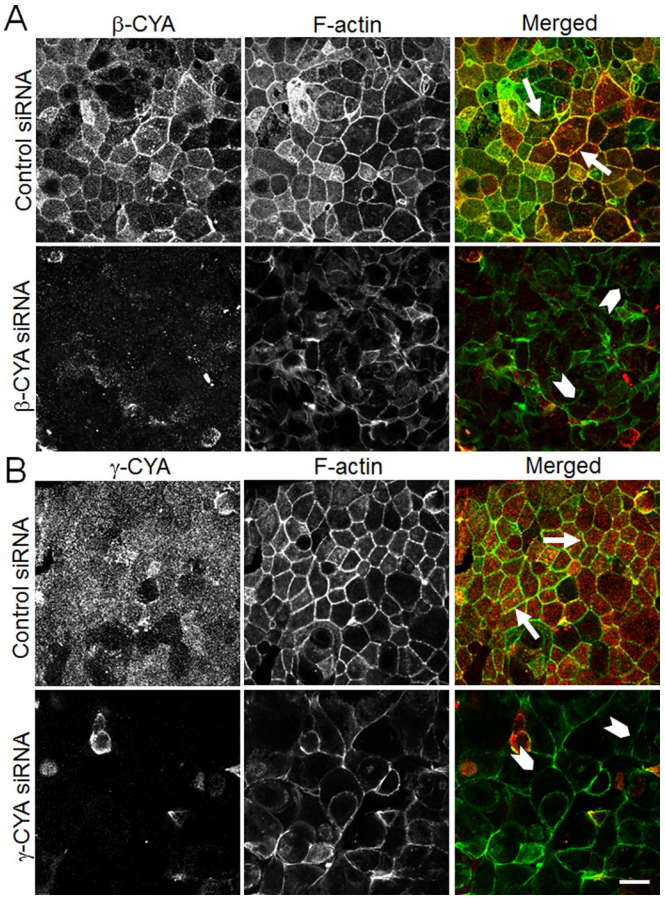

FIGURE 9: Down-regulation of β-CYA and γ-CYA attenuates assembly of the perijunctional actin cytoskeleton. Fluorescence labeling shows rapid formation of the circumferential F-actin belt at the level of apical junctions of control SK-CO15 cells after 3 h of calcium repletion (arrows). By contrast, β-CYA– (A) and γ-CYA–depleted (B) cells demonstrate decreased thickness and labeling intensity of perijunctional F-actin bundles (arrowheads). Scale bar, 20 μm.

less-organized 3D spheroids that are largely devoid of internal lumen (Ivanov *et al.*, 2008). In well-polarized Caco-2 cells, β-CYA and γ-CYA demonstrated differential localization at the AJC that resembled their localization in SK-CO15 monolayers (Supplemental Figure S10). Similar to SK-CO15 cells, siRNA-mediated knockdown resulted in a marked and specific decrease in the expression of cytoplasmic actins in Caco-2 cells (Figure 11A). Control Caco-2 cells growing in Matrigel formed spherical cysts with well-defined internal lumen that was delineated by apical EBP50 labeling and thick F-actin bundles (Figure 11B, arrows). Formation of such hollow cysts was significantly inhibited in β-CYA– or γ-CYA–depleted cells (Figure 11, B and C). Instead, actin isoform–deficient Caco-2 cells primarily grow as spheroids without noticeable lumen and with the apical EBP50 mislocalized to the cyst surface (Figure 11, B and C). These results suggest that both β-CYA and γ-CYA are required for the formation of polarized cysts that represent an early stage of 3D epithelial morphogenesis.

DISCUSSION

β-CYA and γ-CYA regulate maintenance of different junctional complexes and cooperate in establishing the epithelial barrier

The actin cytoskeleton is known to be critical for preserving integrity of the epithelial barrier as well as for remodeling of the AJC during embryonic morphogenesis and in disease states (Yonemura *et al.*, 1995; Mege *et al.*, 2006; Ivanov, 2008; Ivanov *et al.*, 2010a; Cavey and Lecuit, 2009). Previous studies probed the roles of F-actin in AJC biogenesis primarily by altering polymerization status of actin filaments. Here we present the first evidence that intracellular actin level is an important regulator of epithelial junctions and that both cytoplasmic actin isoforms are essential for various aspects of AJC remodeling. One of the most interesting findings of this study is a selective functional coupling of actin isoforms with distinct junctional complexes. Specifically, β-CYA appears to be essential for maintenance of AJs and is dispensable for the normal TJ structure, whereas γ-CYA is important for TJ integrity but plays no obvious role in maintenance of AJs (Figures 4 and 5 and Supplemental Figure S3). A selective impairment of AJs but not TJs in β-CYA–depleted epithelial cells is surprising, given the current dogma that AJs are necessary for proper assembly of other junctional complexes (Gumbiner, 2005; Ogita and Takai, 2006; Hartsock and Nelson, 2008). However, these results are consistent with previous reports that E-cadherin depletion did not prevent the establishment of TJs in renal epithelium (Capaldo and Macara, 2007) and that a clone of HepG2 cells that is unable to make AJs can still assemble TJs (Theard *et al.*, 2007). Of interest, despite having intact TJs, β-CYA–depleted epithelial cells have shown significant defects in apicobasal cell polarity

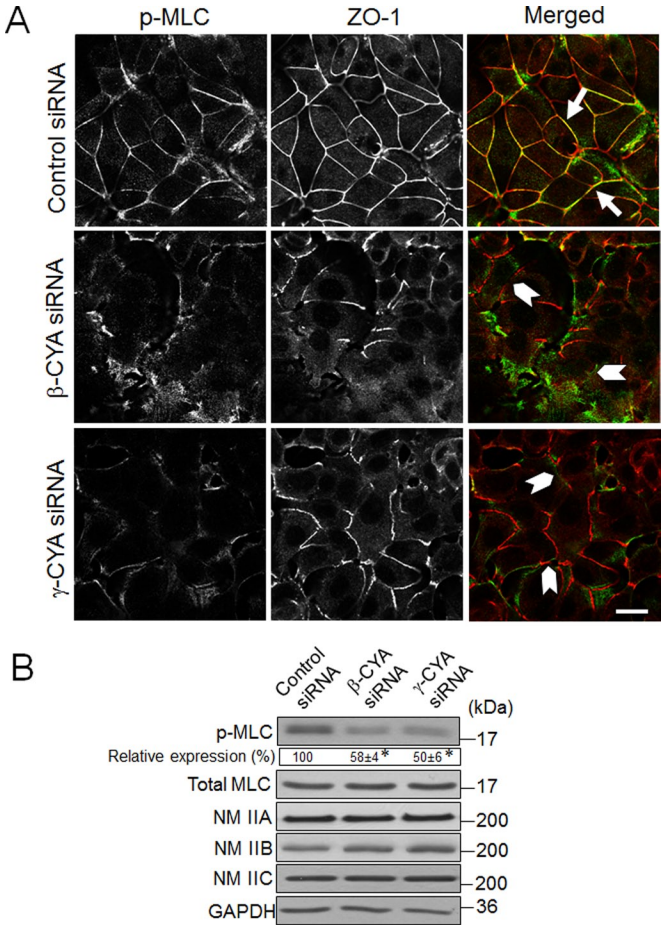

FIGURE 10: Down-regulation of β-CYA and γ-CYA inhibits activation of perijunctional NM II. (A) Immunofluorescence labeling shows significant accumulation of monophosphorylated myosin light chain (p-MLC) at newly assembled TJs in control SK-CO15 cells after 3 h of calcium repletion (arrows). By contrast, little accumulation of p-MLC at the areas of cell–cell contacts can be seen in either β-CYA– or γ-CYA–depleted cells (arrowheads). Scale bar, 20 μm. (B) Immunoblotting analysis shows the decreased cellular level of p-MLC in β-CYA– or γ-CYA–depleted SK-CO15 cells, whereas expression of total MLC, as well as NM II heavy chains A–C, remains unchanged. Data are presented as mean ± SE ($n = 3$); *$p < 0.05$, compared to control siRNA–transfected cells.

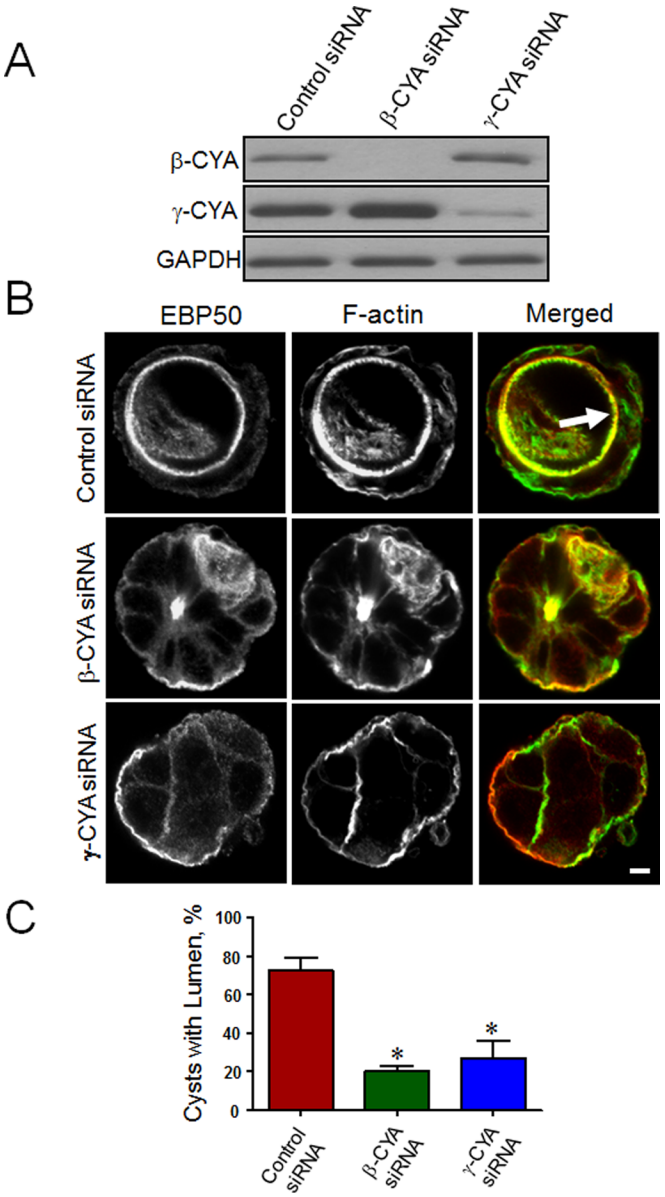

FIGURE 11: Knockdown of β-CYA and γ-CYA disrupts formation of intestinal epithelial cysts. (A) Immunoblotting analysis showing efficient knockdown of individual cytoplasmic actin isoform in Caco-2 cells. (B, C) Representative confocal images and quantitative analysis show formation of polarized cysts with well-defined lumen (arrow) in control siRNA–transfected Caco-2 cells embedded into 3D Matrigel. By contrast, formation of such hollow cysts was inhibited in Matrigel-growing β-CYA– or γ-CYA–depleted Caco-2 cells. Data are presented as mean ± SE ($n = 3$); *$p < 0.05$, compared to control siRNA–transfected cells. Scale bar, 5 μm.

(Figure 6A). Furthermore, loss of β-CYA selectively disrupted the characteristic perijunctional labeling of Par-3 (Figure 6C), which suggests that mislocalization of Par-3 can contribute to the observed defects in epithelial cell polarity. Because Par-3 is a known regulator of TJs (Suzuki and Ohno, 2006; McCaffrey and Macara, 2009), it seems unusual to observe intact TJs in β-CYA–depleted cells with mislocalized Par-3. However, our findings are consistent with previously observed effects of Par-3 knockdown, which did not disrupt a steady-state TJ structure but attenuated TJ reassembly in renal epithelial cells (Chen and Macara, 2005). An additional mechanism of impaired apicobasal polarity in β-CYA–depleted epithelia may involve disrupted vesicle trafficking from the Golgi to the plasma membrane. This suggestion is supported by data on the F-actin dependence of vesicle exocytosis (Hirschberg *et al.*, 1998) and localization of β-CYA in the Golgi and Golgi-derived carrier vesicles (Valderrama *et al.*, 2000).

Of importance, depletion of either β-CYA or γ-CYA increased the permeability of model intestinal epithelial cell monolayers (Figure 3, C and D), supporting the idea that AJs and TJs cooperate in the establishment of the epithelial barrier. Two distinct paracellular permeability pathways have been identified in simple epithelia. The first–the pore pathway–mediates passage of small ions with molecular radius not exceeding 4 Å and can be evaluated by measuring TEER (Watson *et al.*, 2001; Van Itallie *et al.*, 2010). The second pathway—transepithelial leak—that mediates passage of large molecules with variable sizes can be probed by measuring fluxes of different marker molecules. β-CYA or γ-CYA appears to control both paracellular pathways, since depletion of individual actin isoforms

decreased TEER and increased dextran fluxes in SK-CO15 cell monolayers (Figure 3, C and D). Given the dramatic increase in epithelial permeability after either β-CYA or γ-CYA knockdown, one can predict that depletion of cytoplasmic actin isoforms in vivo would lead to dramatic abnormalities in epithelial organization and/or functions. This may be true for β-CYA depletion, since β-CYA hypomorphic mice are embryonically lethal (Shawlot *et al.*, 1998). By contrast, γ-CYA–null mice do not display gross developmental abnormalities, although they die at 48 h after birth due to respiratory distress (Belyantseva *et al.*, 2009; Bunnell and Ervasti, 2010). However, it is not unusual for epithelial tissues to develop normally while having defective TJ functions. For example, mice genetically deficient in a key TJ protein, junctional adhesion molecule A, do not show any vivid physiologic abnormalities despite having increased permeability of the intestinal epithelium (Laukoetter *et al.*, 2007).

In a cell-free actin polymerization assay, β-CYA or γ-CYA has been shown to readily copolymerize and create mixed isoform filaments (Bergeron *et al.*, 2010). However, our data suggest that the perijunctional cytoskeleton of epithelial cells contains a substantial proportion of single-isoform filaments composed of either β-CYA or γ-CYA. Such filaments are spatially segregated during early steps of cell–cell contact assembly, where β-CYA–based filaments are associated with newly formed junctions, whereas distinct γ-CYA–based filaments run in parallel to the adhesive contacts (Figure 1). This topography closely resembles two F-actin populations previously observed at calcium-dependent intercellular junctions in keratinocytes (Zhang *et al.*, 2005) and may reflect differences in their functions. Specifically, β-CYA filaments may control assembly of adhesive E-cadherin clusters, whereas γ-CYA filaments are likely to mediate alignment and expansion of initial cell–cell contacts. During maturation of epithelial contacts and TJ assembly, β-CYA and γ-CYA filaments coalesce and became microscopically poorly distinguishable, but they still possess unique biochemical features. Indeed, results of our Lat B test revealed the existence of stable, γ-CYA–based filaments at the mature AJC, whereas perijunctional β-CYA–rich actin bundles appeared to be more dynamic (Figure 2). These findings are consistent with recently reported differences in polymerization dynamics of cytoplasmic actins in a cell-free system (Bergeron *et al.*, 2010). In a test tube, β-CYA demonstrated much quicker rates of polymerization and depolymerization compared to those of γ-CYA, thereby indicating decreased stability of β-CYA filaments. Because β-CYA is known to be enriched in cellular structures that undergo rapid remodeling (Hoock *et al.*, 1991; Zhang *et al.*, 1999), its high mobility can serve as an important regulator of cellular plasticity.

β-CYA and γ-CYA cooperate in rapid reassembly of apical junctions and formation of three-dimensional epithelial cysts

AJs and TJs are known to undergo a rapid remodeling (disassembly and reassembly) in normal epithelial morphogenesis and during disease-related breakdown of mucosal barriers (Yan *et al.*, 2008; Cavey and Lecuit, 2009; Ivanov *et al.*, 2010a; Niessen *et al.*, 2011; Shen *et al.*, 2011). Evidence suggests that molecular mechanisms controlling the AJC remodeling can be different from the mechanisms that mediate maintenance of the mature junctions (Capaldo and Macara, 2007; Naydenov and Ivanov, 2010). In line with this idea, we found that both β-CYA and γ-CYA are essential for the rapid calcium-stimulated reassembly of AJs and TJs. This conclusion is based on the effects of siRNA-mediated knockdown of individual actin isoforms (Figures 7 and 8) and isoform-specific inhibitory peptides (Supplemental Figures S8 and S9). The peptide data are important since they indicate that attenuated AJ/TJ reassembly in β-CYA– or γ-CYA–depleted cells is not due to insufficient total level of monomeric actin to achieve the efficient actin filament assembly. Similarly, our finding that knockdown of individual actin isoforms did not prevent junctional disruption in calcium-depleted cells (Supplemental Figure S6) also indicates that β-CYA– or γ-CYA–depleted cells retain a sufficient level of actin protein to mediate the cytoskeleton-driven AJC remodeling.

The attenuated AJ/TJ reassembly in β-CYA– or γ-CYA–depleted SK-CO15 cells is likely to be a consequence of the defective formation of the contractile perijunctional actomyosin belt (Figures 9 and 10 and Supplemental Figure S9). Such cytoskeletal abnormalities could impair reformation of AJs and TJs by two different mechanisms. One mechanism is loss of F-actin–dependent stabilization of junctional complexes that results in their rapid endocytosis (Shen and Turner, 2005). The other mechanism is a diminished actomyosin contractility that impedes expansion of initial cell–cell contacts and formation of circumferential AJs and TJs (Ivanov *et al.*, 2005, 2007; Shewan *et al.*, 2005; Zhang *et al.*, 2005; Smutny *et al.*, 2010). Of interest, loss of either β-CYA or γ-CYA caused similar decrease in total amount of p-MLC (Figure 10B). This indicates that both β-CYA and γ-CYA filaments are capable of activating NM II motors and mediating contractile processes during formation of epithelial cell–cell contacts.

Our study suggests that β-CYA and γ-CYA not only cooperate in regulating structure and functions of planar epithelial monolayers, but they also work together in mediating early steps of 3D epithelial morphogenesis. Indeed, loss of either actin isoform dramatically attenuated formation of hollow cysts by Matrigel-embedded Caco-2 cells (Figure 11B). It is noteworthy that β-CYA depletion impaired apicobasal cell polarity both in 3D cysts and planar cell monolayers, whereas γ-CYA knockdown caused polarity defects only in the 3D system. Overall our findings reinforce a current view on the actomyosin cytoskeleton as a key determinant of formation of 3D epithelial structures (Yu *et al.*, 2008; Qin *et al.*, 2010; Kovacs *et al.*, 2011) and reveal β-CYA and γ-CYA as important molecular players in this process.

Given a remarkable similarity in β-CYA and γ-CYA structure, it is important to understand what can determine their differential cellular distribution and nonredundant functions. Several mechanisms have been proposed to explain unique cellular roles of cytoplasmic actins. First is a unique posttranscriptional modification of β-CYA that involves its arginylation at the Asp3 residue (Karakozova *et al.*, 2006). Arginylation of β-CYA was shown to alter its biochemical properties by preventing excessive aggregation of β-CYA polymers (Karakozova *et al.*, 2006; Saha *et al.*, 2010). Because such modification was shown to affect actin-dependent cell motility (Karakozova *et al.*, 2006), it would be interesting to examine whether arginylation of perijunctional β-CYA can regulate remodeling of epithelial AJs and TJs. Another mechanism that explains different biochemical characteristics and cellular functions of β-CYA and γ-CYA implies their association with distinct subsets of actin-binding proteins (Perrin and Ervasti, 2010). For example, annexin 5a was shown to preferentially associate with γ-CYA (Tzima *et al.*, 2000), whereas ezrin and βCAP73 are believed to have predominant affinity for β-CYA filaments (Shuster and Herman, 1995; Shuster *et al.*, 1996).

In conclusion, this study provides the first evidence that two cytoplasmic actin isoforms play nonredundant roles in regulating the AJC in model intestinal epithelia. β-CYA appears to be essential for maintenance of mature AJs and apicobasal cell polarity, whereas γ-CYA controls normal TJ architecture. The functional interplay between these isoforms is important for normal paracellular permeability, rapid calcium-dependent AJ/TJ reassembly, and formation of three-dimensional epithelial cysts. Future studies are warranted to provide additional insights into mechanisms and biological roles

of cytoplasmic actins during normal epithelial morphogenesis and in different disease states.

MATERIALS AND METHODS

Antibodies and other reagents

The following primary polyclonal (pAb) and monoclonal (mAb) antibodies were used to detect junctional, cytoskeletal, and signaling proteins: anti–occludin, ZO-1, claudin-1, claudin-4, and JAM-A mAbs and pAbs (Invitrogen, Carlsbad, CA); anti–PARP, caspase-3, total MLC, phospho-MLC, NM IIC, phospho-PKCζ, and glyceraldehyde-3-phosphate dehydrogenase pAbs (Cell Signaling, Danvers, MA); anti–E-cadherin, β-catenin, p120 catenin, PKCι, and afadin mAbs (BD Biosciences, San Jose, CA); anti-EBP50 mAb (Abcam); anti–NM IIA and NM IIB pAbs (Covance, Princeton, NJ); anti–β-catenin pAb (Sigma-Aldrich, St. Louis, MO); anti–total PKCζ and PAR-6 pAbs (Santa Cruz Biotechnology, Santa Cruz, CA); and anti–Par-3 pAb (EMD-Millipore, Billerica, MA). Monoclonal antibodies selectively recognizing β-CYA and γ-CYA were described previously (Dugina *et al.*, 2009). Alexa 488 or Alexa 555 dye–conjugated donkey anti-rabbit and goat anti-mouse secondary antibodies, as well as Alexa dye–conjugated phalloidin, were obtained from Invitrogen. FITC-labeled mouse immunoglobulin G1 (IgG1) and tetramethylrhodamine isothiocyanate–labeled mouse IgG2b secondary antibodies were purchased from Southern Biotech (Birmingham, AL). Horseradish peroxidase–conjugated goat anti-rabbit and anti-mouse secondary antibodies were purchased from Bio-Rad Laboratories (Hercules, CA). Latrunculin B was purchased from EMD-Millipore. All other reagents were obtained from Sigma-Aldrich.

Cell culture and calcium switch model

SK-CO15 (a gift from E. Rodriguez-Boulan, Weill Medical College of Cornell University, Ithaca, NY) and Caco-2 BBE (American Type Culture Collection, Manassas, VA) human colonic epithelial cells were cultured as previously described (Le Bivic *et al.*, 1989; Ivanov *et al.*, 2007, 2008; Naydenov *et al.*, 2009; Naydenov and Ivanov, 2010). Cells were grown in standard T75 flasks and for immunolabeling/confocal microscopy experiments were seeded on either collagen-coated, permeable polycarbonate filters (0.4 µm pore size; Costar, Cambridge, MA) or collagen-coated coverslips. For biochemical experiments, the cells were seeded on six-well plastic plates. To study AJ/TJ disassembly and reassembly, we subjected confluent SK-CO15 cells to the calcium switch as previously described (Ivanov *et al.*, 2004, 2005; Naydenov *et al.*, 2009).

Immunofluorescence labeling and image analysis

Immunolabeling of β-CYA and γ-CYA was performed as described previously (Dugina *et al.*, 2009). Briefly, epithelial cell monolayers were fixed with prewarmed 1% paraformaldehyde (PFA) in DMEM for 30 min, followed by 5 min of permeabilization with methanol at –20°C. In some experiments involving immunolabeling of AJ/TJ proteins, cells were fixed/permeabilized in 100% methanol for 20 min at –20°C. For detergent preextraction, confluent SK-CO15 cells were incubated with a cytoskeleton-stabilization buffer (0.5% Triton X-100, 10 mM 2-(*N*-morpholino) ethanesulfonic acid, 138 mM KCl, 3 mM $MgCl_2$, 2 mM ethylene glycol tetraacetic acid [EGTA], 0.32 mM sucrose, and 1 µg/ml phalloidin) for 15 min on ice. Fixed cells were blocked in 4-(2-hydroxyethyl)-1-piperazineethanesulfonic acid (HEPES)–buffered Hank's balanced salt solution ($HBSS^+$) containing 1% bovine serum albumin (blocking buffer) for 60 min at room temperature and incubated for another 60 min with primary antibodies diluted in the blocking buffer. Cells were then washed, incubated for 60 min with Alexa dye–conjugated secondary antibodies, rinsed with blocking buffer, and mounted on slides with ProLong Antifade medium (Invitrogen, Carlsbad, CA). Immunofluorescently labeled cell monolayers were examined using an Olympus FluoView 1000 confocal microscope (Olympus America, Center Valley, PA). The Alexa Fluor 488 and 555 signals were imaged sequentially in frame-interlace mode to eliminate cross-talk between channels. The images were processed using the Olympus FV10-ASW 2.0 Viewer software and Photoshop (Adobe, San Jose, CA). Images shown are representative of at least three experiments, with multiple images taken per slide.

Peptide inhibition experiments

FITC-labeled, TAT-conjugated, cell-permeable inhibitory peptides for β-CYA (Ac-DDDIA), γ-CYA (Ac-EEEIA), and α-SMA (Ac-DEDE) were synthesized as previously described (Kim *et al.*, 2008). To analyze effects of the peptides on AJ/TJ reassembly, confluent SK-CO15 cells were subjected to overnight calcium depletion, followed by additional 1 h incubation with 20 µM of individual inhibitory peptide dissolved in a low-calcium medium. Afterward, the cells were subjected to 3 h of calcium repletion in the presence of the same concentration of the peptide. Cells incubated without peptides or exposed to 20 µM α-SMA peptide were used as controls. Cell monolayers were fixed with 4% PFA, permeabilized with 0.5% Triton X-100, and stained for AJ/TJ proteins as described.

Immunoblotting

Cells were homogenized in RIPA lysis buffer (20 mM Tris, 50 mM NaCl, 2 mM EDTA, 2 mM EGTA, 1% sodium deoxycholate, 1% Triton X-100, and 0.1% SDS, pH 7.4), containing a protease inhibitor cocktail (1:100; Sigma-Aldrich) and phosphatase inhibitor cocktails 1 and 2 (both at 1:200; Sigma-Aldrich). Lysates were cleared by centrifugation (20 min at 14,000 × *g*), diluted with 2× SDS sample buffer, and boiled. SDS–PAGE and immunoblotting were conducted by standard protocols with an equal amount of total protein (10 or 20 µg) per lane. Protein expression was quantified by densitometry of three immunoblot images, each representing an independent experiment, with a Kodak Image Station 2000R and Kodak Molecular Imaging software, version 4.0 (Eastman Kodak, Rochester, NY). Data are presented as normalized values assuming the expression levels in control siRNA–treated groups were at 100%. Statistical analyses were performed with row densitometric data using Excel (Microsoft, Redmond, WA).

RNA interference

The siRNA-mediated knockdown of actin isoforms in SK-CO15 and Caco-2 epithelial cells was carried out as previously described (Ivanov *et al.*, 2007; Naydenov and Ivanov, 2010). Individual siRNA duplexes targeting the human β-CYA (duplex 1, GGGCAUGGGUCAGAAGGAU; duplex 2, AAACCUAACUUGCGCAGAA) and γ-CYA (duplex 1, GAGAAGAUGACUCAGAUUA; duplex 2, GAGCCGUGUUUCCUUCCAU) were purchased from Dharmacon (Lafayette, CO). A noncoding siRNA duplex 2 was used as a control. Cells were transfected using the DharmaFect 1 reagent (Dharmacon) in Opti-MEM I medium (Invitrogen) according to the manufacturer's protocol with a final siRNA concentration of 50 nM. Cells were used in experiments on days 3 and 4 posttransfection.

Epithelial cyst formation in Matrigel

Three-dimensional epithelial cyst assay was performed as described in detail previously (Ivanov *et al.*, 2008). Briefly, Caco-2 cell were transfected with either control or actin isoform–specific siRNAs, and the next day cells were trypsinized, resuspended in DMEM,

and mixed with a growth factor–reduced Matrigel (BD Biosciences, San Jose, CA). Matrigel-embedded cells were plated in Lab-Tek 16-well chamber glass systems (Nagle, Rochester, NY). Cysts were allowed to form for 72 h at 37°C; 1 μM forskolin was present during the last 24 h to enhance cyst lumen formation. Cysts were fixed in 4% PFA, permeabilized with 0.5% Triton X-100, and stained using a standard protocol, except that blocking, primary, and secondary antibody incubation were performed for 2 h, and all washing steps were performed for 30 min. For the quantitative analysis, cyst images were acquired at low resolution, and total number of cysts and number of cysts with the lumen were counted manually.

Epithelial barrier permeability measurements

TEER was measured with an EVOMX voltohmmeter (World Precision Instruments, Sarasota, FL). The resistance of cell-free collagen-coated filters was subtracted from each experimental point. Dextran flux assay was performed as described (Ivanov *et al.*, 2010b). Briefly, on day 4 after siRNA transfection, SK-CO15 cell monolayers growing on the Transwell filter were exposed to 1 mg/ml of either FITC dextran 4000 Da or 40,000 Da in HBSS added to the upper chamber, whereas HBSS only was added to the lower chamber. After 60 min of incubation, HBSS samples were collected from the lower chamber, and FITC fluorescence intensity was measured using a Victor V plate reader (Applied Biosystems, Carlsbad, CA) with excitation and emission wavelengths 485 and 544 nm, respectively. After subtraction of fluorescence of the dextran-free HBSS, relative intensity was calculated by using Prism 5 software (GraphPad, La Jolla, CA).

Statistics

Numerical values from individual experiments were pooled and expressed as mean ± SEM throughout. The numbers obtained were compared by two-tailed Student's *t* test, with statistical significance assumed at $p < 0.05$.

ACKNOWLEDGMENTS

We thank E. Rodriguez-Boulan for providing SK-CO15 cells for this study. This work was supported by National Institutes of Health Grants RO1 DK083968 and R01 DK084953 to A.I.I. and P01 HL86655 to K.G.M. and by Swiss National Science Foundation Grant 310030_125320 to C.C.

REFERENCES

Abe K, Takeichi M (2008). EPLIN mediates linkage of the cadherin catenin complex to F-actin and stabilizes the circumferential actin belt. Proc Natl Acad Sci USA 105, 13–19.

Ammar DA, Nguyen PN, Forte JG (2001). Functionally distinct pools of actin in secretory cells. Am J Physiol Cell Physiol 281, C407–C417.

Anderson JM, Van Itallie CM (2009). Physiology and function of the tight junction. Cold Spring Harb Perspect Biol 1, a002584.

Ayscough K (1998). Use of latrunculin-A, an actin monomer-binding drug. Methods Enzymol 298, 18–25.

Belyantseva IA *et al.* (2009). γ-Actin is required for cytoskeletal maintenance but not development. Proc Natl Acad Sci USA 106, 9703–9708.

Bentzel CJ, Hainau B, Ho S, Hui SW, Edelman A, Anagnostopoulos T, Benedetti EL (1980). Cytoplasmic regulation of tight-junction permeability: effect of plant cytokinins. Am J Physiol 239, C75–C89.

Bergeron SE, Zhu M, Thiem SM, Friderici KH, Rubenstein PA (2010). Ion-dependent polymerization differences between mammalian β- and γ-nonmuscle actin isoforms. J Biol Chem 285, 16087–16095.

Bunnell TM, Burbach BJ, Shimizu Y, Ervasti JM (2011). β-Actin specifically controls cell growth, migration, and the G-actin pool. Mol Biol Cell 22, 4047–4058.

Bunnell TM, Ervasti JM (2010). Delayed embryonic development and impaired cell growth and survival in Actg1 null mice. Cytoskeleton (Hoboken) 67, 564–572.

Capaldo CT, Macara IG (2007). Depletion of E-cadherin disrupts establishment but not maintenance of cell junctions in Madin-Darby canine kidney epithelial cells. Mol Biol Cell 18, 189–200.

Cavey M, Lecuit T (2009). Molecular bases of cell-cell junctions stability and dynamics. Cold Spring Harb Perspect Biol 1, a002998.

Cavey M, Rauzi M, Lenne PF, Lecuit T (2008). A two-tiered mechanism for stabilization and immobilization of E-cadherin. Nature 453, 751–756.

Chen X, Macara IG (2005). Par-3 controls tight junction assembly through the Rac exchange factor Tiam1. Nat Cell Biol 7, 262–269.

Dugina V, Zwaenepoel I, Gabbiani G, Clement S, Chaponnier C (2009). β- and γ-cytoplasmic actins display distinct distribution and functional diversity. J Cell Sci 122, 2980–2988.

Dugina VB, Chipysheva TA, Ermilova VD, Gabbiani D, Chaponnier C, Vasil'ev Iu M (2008). Distribution of actin isoforms in normal, dysplastic, and tumorous human breast cells [in Russian]. Arkh Patol 70, 28–31.

Durgan J, Kaji N, Jin D, Hall A (2011). Par6B and atypical PKC regulate mitotic spindle orientation during epithelial morphogenesis. J Biol Chem 286, 12461–12474.

Giepmans BN, van Ijzendoorn SC (2009). Epithelial cell-cell junctions and plasma membrane domains. Biochim Biophys Acta 1788, 820–831.

Green KJ, Getsios S, Troyanovsky S, Godsel LM (2010). Intercellular junction assembly, dynamics, and homeostasis. Cold Spring Harb Perspect Biol 2, a000125.

Gumbiner BM (2005). Regulation of cadherin-mediated adhesion in morphogenesis. Nat Rev Mol Cell Biol 6, 622–634.

Hartsock A, Nelson WJ (2008). Adherens and tight junctions: structure, function and connections to the actin cytoskeleton. Biochim Biophys Acta 1778, 660–669.

Hinz B, Gabbiani G, Chaponnier C (2002). The NH2-terminal peptide of α-smooth muscle actin inhibits force generation by the myofibroblast in vitro and in vivo. J Cell Biol 157, 657–663.

Hirokawa N, Keller TC 3rd, Chasan R, Mooseker MS (1983). Mechanism of brush border contractility studied by the quick-freeze, deep-etch method. J Cell Biol 96, 1325–1336.

Hirokawa N, Tilney LG (1982). Interactions between actin filaments and between actin filaments and membranes in quick-frozen and deeply etched hair cells of the chick ear. J Cell Biol 95, 249–261.

Hirschberg K, Miller CM, Ellenberg J, Presley JF, Siggia ED, Phair RD, Lippincott-Schwartz J (1998). Kinetic analysis of secretory protein traffic and characterization of Golgi to plasma membrane transport intermediates in living cells. J Cell Biol 143, 1485–1503.

Hoock TC, Newcomb PM, Herman IM (1991). β Actin and its mRNA are localized at the plasma membrane and the regions of moving cytoplasm during the cellular response to injury. J Cell Biol 112, 653–664.

Ivanov AI (2008). Actin motors that drive formation and disassembly of epithelial apical junctions. Front Biosci 13, 6662–6681.

Ivanov AI, Bachar M, Babbin BA, Adelstein RS, Nusrat A, Parkos CA (2007). A unique role for nonmuscle myosin heavy chain IIA in regulation of epithelial apical junctions. PLoS One 2, e658.

Ivanov AI, Hopkins AM, Brown GT, Gerner-Smidt K, Babbin BA, Parkos CA, Nusrat A (2008). Myosin II regulates the shape of three-dimensional intestinal epithelial cysts. J Cell Sci 121, 1803–1814.

Ivanov AI, Hunt D, Utech M, Nusrat A, Parkos CA (2005). Differential roles for actin polymerization and a myosin II motor in assembly of the epithelial apical junctional complex. Mol Biol Cell 16, 2636–2650.

Ivanov AI, McCall IC, Parkos CA, Nusrat A (2004). Role for actin filament turnover and a myosin II motor in cytoskeleton-driven disassembly of the epithelial apical junctional complex. Mol Biol Cell 15, 2639–2651.

Ivanov AI, Parkos CA, Nusrat A (2010a). Cytoskeletal regulation of epithelial barrier function during inflammation. Am J Pathol 177, 512–524.

Ivanov AI, Young C, Den Beste K, Capaldo CT, Humbert PO, Brennwald P, Parkos CA, Nusrat A (2010b). Tumor suppressor scribble regulates assembly of tight junctions in the intestinal epithelium. Am J Pathol 176, 134–145.

Karakozova M, Kozak M, Wong CC, Bailey AO, Yates JR 3rd, Mogilner A, Zebroski H, Kashina A (2006). Arginylation of β-actin regulates actin cytoskeleton and cell motility. Science 313, 192–196.

Khaitlina SY (2001). Functional specificity of actin isoforms. Int Rev Cytol 202, 35–98.

Kim HR, Gallant C, Leavis PC, Gunst SJ, Morgan KG (2008). Cytoskeletal remodeling in differentiated vascular smooth muscle is actin isoform dependent and stimulus dependent. Am J Physiol Cell Physiol 295, C768–C778.

Kovacs EM, Verma S, Thomas SG, Yap AS (2011). Tuba and N-WASP function cooperatively to position the central lumen during epithelial cyst morphogenesis. Cell Adh Migr 5, 344–350.

Laukoetter MG *et al.* (2007). JAM-A regulates permeability and inflammation in the intestine in vivo. J Exp Med 204, 3067–3076.
Le Bivic A, Real FX, Rodriguez-Boulan E (1989). Vectorial targeting of apical and basolateral plasma membrane proteins in a human adenocarcinoma epithelial cell line. Proc Natl Acad Sci USA 86, 9313–9317.
Liu N, Academia K, Rubio T, Wehr T, Yeck T, Jordan L, Hamby K, Paulus A (2007). Actin deficiency induces cofilin phosphorylation: proteome analysis of HeLa cells after β-actin gene silencing. Cell Motil Cytoskeleton 64, 110–120.
Ma TY, Hollander D, Tran LT, Nguyen D, Hoa N, Bhalla D (1995). Cytoskeletal regulation of Caco-2 intestinal monolayer paracellular permeability. J Cell Physiol 164, 533–545.
Ma TY, Tran D, Hoa N, Nguyen D, Merryfield M, Tarnawski A (2000). Mechanism of extracellular calcium regulation of intestinal epithelial tight junction permeability: role of cytoskeletal involvement. Microsc Res Tech 51, 156–168.
Madara JL (1987). Intestinal absorptive cell tight junctions are linked to cytoskeleton. Am J Physiol 253, C171–C175.
Madara JL, Barenberg D, Carlson S (1986). Effects of cytochalasin D on occluding junctions of intestinal absorptive cells: further evidence that the cytoskeleton may influence paracellular permeability and junctional charge selectivity. J Cell Biol 102, 2125–2136.
Matsumura F (2005). Regulation of myosin II during cytokinesis in higher eukaryotes. Trends Cell Biol 15, 371–377.
McCaffrey LM, Macara IG (2009). Widely conserved signaling pathways in the establishment of cell polarity. Cold Spring Harb Perspect Biol 1, a001370.
Mege RM, Gavard J, Lambert M (2006). Regulation of cell-cell junctions by the cytoskeleton. Curr Opin Cell Biol 18, 541–548.
Meng W, Takeichi M (2009). Adherens junction: molecular architecture and regulation. Cold Spring Harb Perspect Biol 1, a002899.
Micheva KD, Vallee A, Beaulieu C, Herman IM, Leclerc N (1998). β-Actin is confined to structures having high capacity of remodelling in developing and adult rat cerebellum. Eur J Neurosci 10, 3785–3798.
Morton WM, Ayscough KR, McLaughlin PJ (2000). Latrunculin alters the actin-monomer subunit interface to prevent polymerization. Nat Cell Biol 2, 376–378.
Naydenov NG, Hopkins AM, Ivanov AI (2009). c-Jun N-terminal kinase mediates disassembly of apical junctions in model intestinal epithelia. Cell Cycle 8, 2110–2121.
Naydenov NG, Ivanov AI (2010). Adducins regulate remodeling of apical junctions in human epithelial cells. Mol Biol Cell 21, 3506–3517.
Niessen CM, Leckband D, Yap AS (2011). Tissue organization by cadherin adhesion molecules: dynamic molecular and cellular mechanisms of morphogenetic regulation. Physiol Rev 91, 691–731.
Ogita H, Takai Y (2006). Nectins and nectin-like molecules: roles in cell adhesion, polarization, movement, and proliferation. IUBMB Life 58, 334–343.
Perrin BJ, Ervasti JM (2010). The actin gene family: function follows isoform. Cytoskeleton (Hoboken) 67, 630–634.
Perrin BJ, Sonnemann KJ, Ervasti JM (2010). β-Actin and γ-actin are each dispensable for auditory hair cell development but required for stereocilia maintenance. PLoS Genet 6, e1001158.
Qin Y, Meisen WH, Hao Y, Macara IG (2010). Tuba, a Cdc42 GEF, is required for polarized spindle orientation during epithelial cyst formation. J Cell Biol 189, 661–669.
Saha S, Mundia MM, Zhang F, Demers RW, Korobova F, Svitkina T, Perieteanu AA, Dawson JF, Kashina A (2010). Arginylation regulates intracellular actin polymer level by modulating actin properties and binding of capping and severing proteins. Mol Biol Cell 21, 1350–1361.
Schevzov G, Lloyd C, Gunning P (1992). High level expression of transfected β- and γ-actin genes differentially impacts on myoblast cytoarchitecture. J Cell Biol 117, 775–785.
Shawlot W, Deng JM, Fohn LE, Behringer RR (1998). Restricted β-galactosidase expression of a hygromycin-lacZ gene targeted to the β-actin locus and embryonic lethality of β-actin mutant mice. Transgenic Res 7, 95–103.
Shen L, Turner JR (2005). Actin depolymerization disrupts tight junctions via caveolae-mediated endocytosis. Mol Biol Cell 16, 3919–3936.
Shen L, Weber CR, Raleigh DR, Yu D, Turner JR (2011). Tight junction pore and leak pathways: a dynamic duo. Annu Rev Physiol 73, 283–309.
Shewan AM, Maddugoda M, Kraemer A, Stehbens SJ, Verma S, Kovacs EM, Yap AS (2005). Myosin 2 is a key Rho kinase target necessary for the local concentration of E-cadherin at cell-cell contacts. Mol Biol Cell 16, 4531–4542.
Shin K, Fogg VC, Margolis B (2006). Tight junctions and cell polarity. Annu Rev Cell Dev Biol 22, 207–235.
Shuster CB, Herman IM (1995). Indirect association of ezrin with F-actin: isoform specificity and calcium sensitivity. J Cell Biol 128, 837–848.
Shuster CB, Lin AY, Nayak R, Herman IM (1996). βCap73: a novel β actin-specific binding protein. Cell Motil Cytoskeleton 35, 175–187.
Smutny M, Cox HL, Leerberg JM, Kovacs EM, Conti MA, Ferguson C, Hamilton NA, Parton RG, Adelstein RS, Yap AS (2010). Myosin II isoforms identify distinct functional modules that support integrity of the epithelial zonula adherens. Nat Cell Biol 12, 696–702.
Suzuki A, Ohno S (2006). The PAR-aPKC system: lessons in polarity. J Cell Sci 119, 979–987.
Taguchi K, Ishiuchi T, Takeichi M (2011). Mechanosensitive EPLIN-dependent remodeling of adherens junctions regulates epithelial reshaping. J Cell Biol 194, 643–656.
Theard D, Steiner M, Kalicharan D, Hoekstra D, van Ijzendoorn SC (2007). Cell polarity development and protein trafficking in hepatocytes lacking E-cadherin/β-catenin-based adherens junctions. Mol Biol Cell 18, 2313–2321.
Tondeleir D, Vandamme D, Vandekerckhove J, Ampe C, Lambrechts A (2009). Actin isoform expression patterns during mammalian development and in pathology: insights from mouse models. Cell Motil Cytoskeleton 66, 798–815.
Tzima E, Trotter PJ, Orchard MA, Walker JH (2000). Annexin V relocates to the platelet cytoskeleton upon activation and binds to a specific isoform of actin. Eur J Biochem 267, 4720–4730.
Valderrama F, Luna A, Babia T, Martinez-Menarguez JA, Ballesta J, Barth H, Chaponnier C, Renau-Piqueras J, Egea G (2000). The Golgi-associated COPI-coated buds and vesicles contain β/γ-actin. Proc Natl Acad Sci USA 97, 1560–1565.
Vandekerckhove J, Weber K (1978). At least six different actins are expressed in a higher mammal: an analysis based on the amino acid sequence of the amino-terminal tryptic peptide. J Mol Biol 126, 783–802.
Van Itallie CM, Fanning AS, Holmes J, Anderson JM (2010). Occludin is required for cytokine-induced regulation of tight junction barriers. J Cell Sci 123, 2844–2852.
Vasioukhin V, Bauer C, Yin M, Fuchs E (2000). Directed actin polymerization is the driving force for epithelial cell-cell adhesion. Cell 100, 209–219.
Vicente-Manzanares M, Ma X, Adelstein RS, Horwitz AR (2009). Non-muscle myosin II takes centre stage in cell adhesion and migration. Nat Rev Mol Cell Biol 10, 778–790.
Volberg T, Geiger B, Kartenbeck J, Franke WW (1986). Changes in membrane-microfilament interaction in intercellular adherens junctions upon removal of extracellular Ca^{2+} ions. J Cell Biol 102, 1832–1842.
Watson CJ, Rowland M, Warhurst G (2001). Functional modeling of tight junctions in intestinal cell monolayers using polyethylene glycol oligomers. Am J Physiol Cell Physiol 281, C388–C397.
Yan HH, Mruk DD, Cheng CY (2008). Junction restructuring and spermatogenesis: the biology, regulation, and implication in male contraceptive development. Curr Top Dev Biol 80, 57–92.
Yao X, Chaponnier C, Gabbiani G, Forte JG (1995). Polarized distribution of actin isoforms in gastric parietal cells. Mol Biol Cell 6, 541–557.
Yonemura S (2010). Cadherin-actin interactions at adherens junctions. Curr Opin Cell Biol 23, 515–522.
Yonemura S, Itoh M, Nagafuchi A, Tsukita S (1995). Cell-to-cell adherens junction formation and actin filament organization: similarities and differences between non-polarized fibroblasts and polarized epithelial cells. J Cell Sci 108, 127–142.
Yu W, Shewan AM, Brakeman P, Eastburn DJ, Datta A, Bryant DM, Fan QW, Weiss WA, Zegers MM, Mostov KE (2008). Involvement of RhoA, ROCK I and myosin II in inverted orientation of epithelial polarity. EMBO Rep 9, 923–929.
Zhang HL, Singer RH, Bassell GJ (1999). Neurotrophin regulation of β-actin mRNA and protein localization within growth cones. J Cell Biol 147, 59–70.
Zhang J, Betson M, Erasmus J, Zeikos K, Bailly M, Cramer LP, Braga VM (2005). Actin at cell-cell junctions is composed of two dynamic and functional populations. J Cell Sci 118, 5549–5562.